Apolipoprotein A-II is catabolized in the kidney as a function of its plasma concentration

Sonia Dugué-Pujol,[*,†,§] Xavier Rousset,[*,†,§] Danielle Château,[*,†,§] Danièle Pastier,[*,†,§] Christophe Klein,[*,†,§] Jeannine Demeurie,[*,†,§] Charlotte Cywiner-Golenzer,[*,†,§] Michèle Chabert,[*,†,§,] Pierre Verroust,[††] Jean Chambaz,[*,†,§,**] François-Patrick Châtelet,[††] and Athina-Despina Kalopissis[1,*,†,§]**

Institut National de la Santé et de la Recherche Médicale,* U872, Equipe 6, Paris, F-75006 France; Université Pierre et Marie Curie-Paris 6,† UMR S 872, Equipe 6, Paris, F-75006, France; Centre de Recherche des Cordeliers,§ Université Paris Descartes, UMR S 872, Equipe 6, Paris, F-75006, France; Ecole Pratique des Hautes Etudes,** Laboratoire de Pharmacologie Cellulaire et Moléculaire, Paris, F-75006, France and Institut National de la Santé et de la Recherche Médicale,†† U538, CHU Saint Antoine, Paris, F-75012, France

Abstract We investigated in vivo catabolism of apolipoprotein A-II (apo A-II), a major determinant of plasma HDL levels. Like apoA-I, murine apoA-II (mapoA-II) and human apoA-II (hapoA-II) were reabsorbed in the first segment of kidney proximal tubules of control and hapoA-II-transgenic mice, respectively. ApoA-II colocalized in brush border membranes with cubilin and megalin (the apoA-I receptor and coreceptor, respectively), with mapoA-I in intracellular vesicles of tubular epithelial cells, and was targeted to lysosomes, suggestive of degradation. By use of three transgenic lines with plasma hapoA-II concentrations ranging from normal to three times higher, we established an association between plasma concentration and renal catabolism of hapoA-II. HapoA-II was rapidly internalized in yolk sac epithelial cells expressing high levels of cubilin and megalin, colocalized with cubilin and megalin on the cell surface, and effectively competed with apoA-I for uptake, which was inhibitable by anti-cubilin antibodies. Kidney cortical cells that only express megalin internalized LDL but not apoA-II, apoA-I, or HDL, suggesting that megalin is not an apoA-II receptor. We show that apoA-II is efficiently reabsorbed in kidney proximal tubules in relation to its plasma concentration.— Dugué-Pujol, S., X. Rousset, D. Château, D. Pastier, C. Klein, J. Demeurie, C. Cywiner-Golenzer, M. Chabert, P. Verroust, J. Chambaz, F-P. Châtelet, and A-D. Kalopissis. **Apolipoprotein A-II is catabolized in the kidney as a function of its plasma concentration. *J. Lipid Res.* 2007.** 48: **2151–2161.**

Supplementary key words high density lipoprotein • cubilin • megalin • proximal tubule • yolk sac cells • mouse kidney cortical cells • transgenic mice

Apolipoprotein A-I (apoA-I) and apoA-II are the major HDL apolipoproteins and ensure HDL structural stability, because mice deficient in either apoA-I or apoA-II display very low plasma HDL levels (1, 2). Although apoA-I is the most abundant HDL apolipoprotein, the structure and composition of HDL depend in great part on apoA-II, which is more hydrophobic and can displace apoA-I from the surface of native or reconstituted HDL (3, 4). Indeed, the ratio of human apoA-II (hapoA-II)/apoA-I is a key determinant of plasma HDL concentration in hapoA-II-transgenic mice (5, 6). Of note, apoA-II enhances the stability of apoA-I in HDL particles and reduces HDL remodeling by cholesteryl ester transfer protein, probably through the formation of salt bridges between apoA-II and the C-terminal domain of apoA-I (7). Furthermore, apoA-II maintains the plasma HDL pool, in part by inhibiting hepatic lipase activity (8). Because HDL is an independent risk factor for developing cardiovascular artery disease (9, 10), it is important to determine the regulation of plasma apoA-II concentration, a major factor in the control of plasma HDL levels.

Plasma apoA-II content may be regulated by its rates of synthesis and/or catabolism. A kinetic study using stable isotopes has suggested that plasma apoA-II levels are regulated by its rate of synthesis and not by its rate of catabolism (11). The liver is the principal site of apoA-II synthesis (12), but neither the organs catabolizing apoA-II nor the receptor(s) involved have been determined, to our knowledge. We first focused on the kidney as a potential organ of apoA-II catabolism, because it is the major site of apoA-I catabolism in rats, rabbits, and humans (13–17). ApoA-I binds with high affinity to cubilin, a multi-ligand protein

Abbreviations: AMN, amnionless; apoA-II, apolipoprotein A-II; BN, brown Norwegian; DAB, diaminobenzidine; DiI, 1,1′-dioctadecyl-3,3,3′,3′-tetramethylindocarbocyanine; hapoA-II, human apolipoprotein A-II; IF, intrinsic factor; IOD, integrated optical density; mapoA-II, murine apolipoprotein A-II; MKC cells, mouse kidney cortical cells; PFA, paraformaldehyde; SR-BI, scavenger receptor class B type I.

[1] To whom correspondence should be addressed.
e-mail: athina.kalopissis@crc.jussieu.fr

Manuscript received 16 February 2007 and in revised form 5 July 2007.
Published, JLR Papers in Press, July 24, 2007.
DOI 10.1194/jlr.M700089-JLR200

associated with the apical membrane of kidney proximal tubules, intestine, and yolk sac (18–20). However, cubilin lacks a classical transmembrane and cytoplasmic domain necessary for endocytosis, and an accessory protein is necessary to internalize cubilin and its ligands. Conclusive evidence has established that megalin, a member of the LDL receptor family expressed in the same tissues, functions in tandem with cubilin as a coreceptor, cubilin binding to megalin with high affinity (21). Indeed, suppression of megalin activity resulted in inhibition of cubilin-mediated HDL endocytosis (22). Cubilin and megalin share some ligands (albumin, receptor-associated protein, vitamin D binding protein), whereas other ligands are specific either for cubilin [intrinsic factor (IF)-vitamin B_{12}, apoA-I, and HDL, transferrin] or for megalin (apoB, apoE, apoJ, lipoprotein lipase, transcobalamine-vitamine B_{12}) (23).

The objective of the present study was to investigate whether apoA-II is catabolized in the kidney. Because iodination has been shown to artifactually alter in vivo apoA-I catabolism by promoting accelerated catabolism and increasing extra-renal degradation pathways (15), we opted for detecting native apoA-II by immunohistochemistry of kidney sections. This technique offers the additional advantage of visualizing internalized apoA-II in specific cell types. To establish a correlation between the plasma concentration of apoA-II and the extent of its catabolism in the kidney, we used three previously established transgenic mouse lines with hapoA-II plasma concentrations ranging from normal (line β) to two and three times higher (lines δ and λ, respectively) (8). To gain insight into the receptors involved in apoA-II uptake, we studied in vitro apoA-II internalization in rat yolk sac epithelial cells expressing cubilin and megalin and in mouse kidney cortical cells (MKC cells) expressing only megalin.

MATERIALS AND METHODS

Animals

The generation of transgenic mice for hapoA-II has been previously described (7, 8). The three lines, β, δ, and λ, were backcrossed for at least eight generations to strain C57BL/6J (IFFA-CREDO-Charles River). Transgenic mice were detected as described (7, 8) and were hemizygous for the hapoA-II transgene. Male and female control and transgenic mice over 8 weeks of age were used in equal proportions in all studies. The animals were housed in animal rooms with alternating 12 h periods of light (7 AM–7 PM) and dark (7 PM–7AM), and were fed a chow diet (SAFE) with free access to food and water, unless otherwise specified. Blood was drawn from the retroorbital venous plexus or the abdominal vein between 9 AM and 12 AM. For fasting mice, food was withdrawn at 6 PM on the previous day. The procedures followed were in accordance with institutional regulations for the care and use of laboratory animals.

Lipoproteins and apolipoproteins

EDTA-plasma was supplemented with 0.005% gentamycin-1 mM EDTA-0.04% Na-azide and protease inhibitors, and ultracentrifuged to prepare LDL and HDL as described (7, 8). LDL and HDL protein contents were measured (24), and LDL and HDL were labeled with 1,1'-dioctadecyl-3,3,3′,3′-tetramethylindocarbocyanine (DiI) (25). Apolipoproteins were analyzed in plasma, HDL, and urine (collected at 4°C, concentrated 100 times and extensively dialyzed using Amicon Ultra-4 tubes with a 5 kDa cutoff) by 18% SDS-PAGE (26) under nonreducing conditions in order to detect the dimeric form of hapoA-II. After protein transfer to nitrocellulose membranes (0.45 μm; BioRad), hapoA-II was detected by Western blotting using a specific rabbit anti-hapoA-II antibody not recognizing murine apolipoprotein A-II (mapoA-II) (5, 6), and bands were visualized with an alkaline phosphatase substrate system (BioRad).

Immunocytochemical analysis of mouse kidney

Kidneys were quickly removed from control and transgenic mice after intracardiac vascular washing with PBS. Kidney samples were then either frozen in liquid nitrogen after 2 h fixation in 2% paraformaldehyde (PFA) or fixed for 24 h in 4% formalin and embedded in paraffin. Both types of sections (frozen or paraffin-embedded) were processed for immunolocalization. Rabbit anti-mouse apoA-I antibody (Biodesign) was diluted 1/1,500, rabbit anti-mouse apoA-II antibody (Biodesign) was diluted 1/2,000, and rabbit and goat anti-hapoA-II antibodies (courtesy of A. Mazur, National Institute for Agricultural Research) were diluted 1/8,000. Rabbit anti-cubilin and rabbit and sheep anti-megalin antibodies have been described previously (27) and were diluted 1/1,000. Secondary antibodies produced in donkey (Jackson Immunolab; diluted 1/200) were labeled with Cy2 (laser excitation at 488 nm) or Cy3 (543 nm). Double fluorescence images were obtained after mixing of primary antibodies, with appropriate controls. Tissue sections were examined with a laser scanning confocal microscope (Zeiss LSM-510). For conventional bright-field immunomicroscopy, paraffin sections were stained with tyramide amplification (NEN Life Science Products; TSA biotin system NEL700), followed by diaminobenzidine (DAB) precipitation without counterstain.

Histological quantification of apolipoprotein tubular reabsorption

This analysis was conducted with the help of a microscope linked to a computer-based image visualization of DAB-stained paraffin sections. Views of random renal cortical fields at ×25 magnification were digitalized; total number of tubular sections per field was counted; and the number of tubes stained with DAB product signaling apolipoprotein apical reabsorption was noted. Results were expressed as the percentage of stained tubes/total tubes for each group of animals.

Immunoelectron microscopy

Following intracardiac vascular washing with 0.1 M phosphate buffer and fixation of tissues with 4% PFA in 0.1 M phosphate buffer, kidneys of λ-transgenic mice were trimmed and immersion-fixed in 4% PFA in 0.1 M phosphate buffer for 4 h at 4°C. Tissues were dehydrated through graded alcohol, infiltrated in a mixture of ethanol-LRWhite resin (AGAR, R 12 81), and then embedded and polymerized in LRWhite resin at 37°C over 5 days. Ultrathin sections (60 nm) were cut on the ultratome Leica Ultracut UCT, and picked up on Formvar/carbon-coated 300-mesh nickel grids. Immunolabeling with rabbit anti-hapoA-II antibody (1/500) was performed overnight at 4°C and visualized by incubation with donkey anti-rabbit-gold (Aurion; 0.8 nm, DAR ultrasmall, 800.311) diluted 1/100 in PBS, 0.8% BSA, 0.1% fish gelatin, and 15 mM NaN3 for 2 h at room temperature. Sections were postfixed for 10 min in 2.5% glutaraldehyde in PBS, and the gold particles were amplified with Silver Enhancement (Aurion kit R-Gent SE-ME) for 30 min at room tempera-

ture. Finally, the grids were stained with lead citrate and uranyl acetate according to standard procedures, and photographed in a Jeol CX 100 electron microscope.

Purification and labeling of hapoA-II and apoA-I

HapoA-II and apoA-I were purified from delipidated human HDL by preparative isoelectric focusing with a pH gradient of 4–6, and purity was checked by SDS-PAGE in 15% gels. ApoA-II was fluorescently labeled with Alexa 488 and apoA-I with Alexa 546 (Alexa Protein Labeling kits A-10237 and A-10235, respectively; Molecular Probes), according to the manufacturer's instructions.

Cell culture studies

Brown Norwegian (BN) rat yolk sac epithelial cells (BN cells) were derived after fetectomy and placental injection with Moloney's sarcoma virus (28). They were grown in DMEM (Life Technologies) supplemented with 10% fetal calf serum, 1% penicillin, and 1% streptomycin, in 5% CO_2. MKC epithelial cells were derived from SV40-transgenic mice (29). They were routinely cultured in DMEM medium: Ham's F_{12} (1:1; v/v), sodium selenite (2×10^{-8} M), nonessential amino acids, glutamine (4 mM), Hepes (33 mM), $NaHCO_3$ (25 mM), penicillin/streptomycin (50 UI/ml), fungizone (0.25 μg/ml), supplemented with insulin (0.5 μg/ml), triiodothyronin (1 μM), transferrin (5 μg/ml), cholera toxin (10 ng/ml), epidermal growth factor (10 ng/ml), dexamethasone (50 nM), and 5% fetal calf serum. They were seeded on semipermeable filters coated with extracellular matrix basement membrane (matrix-derived from Englebreth-Holm-Swarm mouse tumor; Harbor Bioproducts), and incubated in 5% CO_2 at 37°C.

Uptake of apoA-II by yolk sac cells

BN cells were grown to 90% confluence on 4-chamber borosilicate slides (Nulge Nunc) in DMEM, washed three times in PBS, and incubated in 250 μl serum-free DMEM supplemented with 0.1% BSA. A first kinetic study was performed to investigate apoA-II uptake: Alexa 488-apoA-II and Alexa 546-apoA-I were separately added to a final concentration of 0.25, 0.5, 1, or 2 μg/ml and incubated at 37°C for 1, 5, 15, or 30 min. The cells were washed three times in PBS and fixed in 4% PFA for 30 min, and apolipoprotein internalization was analyzed by confocal microscopy. Internalization of unlabeled hapoA-II and hapoA-I was studied by incubating cells with 0.25 μg/ml of each apolipoprotein at 37°C for 15 min, followed by washes with PBS, fixation in PFA, and permeabilization with 0.1% Triton X-100 in PBS/3% BSA for 5 min. Cells were then washed with PBS containing 100 mM glycine, incubated with PBS at room temperature for 60 min, first with anti-hapoA-II or anti-hapoA-I antibodies (diluted 1/1,000) and then with Cy2- or Cy3-labeled secondary antibodies (diluted 1/200), and analyzed by confocal microscopy. To study colocalization of Alexa-apoA-II and Alexa-apoA-I, the cells were incubated with both apolipoproteins (2 μg/ml each) at 37°C for 1, 5, or 30 min. After three washes with PBS, cells were fixed in 4% PFA, washed with PBS/glycine, and analyzed by confocal microscopy. To study colocalization of apoA-II and apoA-I with cubilin and megalin, cells were incubated at 4°C for 1 h with either Alexa-apoA-II or Alexa-apoA-I (2 μg/ml of each), washed with PBS, fixed in PFA, washed with PBS/glycine and incubated with rabbit anti-cubilin or anti-megalin antibodies (diluted 1/1,000), followed by incubation with Cy2- or Cy3-labeled secondary antibodies (diluted 1/200) and confocal analysis. To establish nonspecific fluorescence, the cells were incubated with unlabeled apoA-II and apoA-I and then with Cy2- and Cy3-labeled secondary antibodies, omitting the primary antibodies. Optical sections were dual-scanned for both green (Alexa 488-apoA-II) and red (Alexa 546-apoA-I) wavelength.

Competition studies of apoA-II internalization in yolk sac cells

To study whether apoA-II competed with apoA-I for internalization, BN cells were incubated at 37°C for 5 min with each Alexa-apolipoprotein alone (0.25 μg/ml) or with either hapoA-I (500-fold excess, mol/mol), hapoA-II (500-fold excess, mol/mol), HDL from control mice (52 μg/ml), HDL from transgenic mice (52 μg/ml), or LDL from control mice (52 μg/ml). To study whether the internalization of apoA-II could be inhibited by anti-cubilin antibodies, cells were incubated at 37°C for 10 min in serum-free DMEM containing rabbit anti-cubilin IgG (100 μg/ml) purified from anti-cubilin antiserum by protein G-Sepharose chromatography (Amersham-Pharmacia Biotechnology) or normal goat IgG (100 μg/ml). Alexa 488-apoA-II was then added, to a final concentration of 0.25 μg/ml, and incubated at 37°C for 5 min. At the end of incubation, the cells were washed three times in PBS, fixed in 4% PFA, washed in PBS/glycine, and analyzed by confocal microscopy, as described above. To quantify fluorescent apolipoprotein uptake in the presence of competitors, stack images of the cells (z axis) were taken using the confocal microscope. For each stack, total fluorescence of the field was estimated as the sum of the integrated optical density (IOD) of each slice measured with Scion Image (Scion Corporation). The mean value of four stacks was used to compare the different conditions.

Confocal microscopic analysis of kidney cortical cells

MKC cells were tested for the presence of cubilin and megalin on their surfaces and for uptake of apoA-II, apoA-I, and LDL. MKC cells were incubated at 37°C with Alexa 488-apoA-II or Alexa 546-apoA-I (1 and 2 μg/ml) for 15 min or 2 h. To study uptake of LDL, cells were incubated with DiI-LDL (2 and 4 μg/ml) for 15 min. At the end of incubation, cells were processed as described above and analyzed by confocal microscopy.

Receptor immunoblot analysis

Membrane proteins of kidney, BN, and MKC cells were prepared as described (30). Membrane extracts (10 μg protein for kidney and BN cell extracts, and 86 μg protein for MKC cell extracts) were analyzed by 4–15% SDS-PAGE. After protein transfer to nitrocellulose membranes (0.45 μm; BioRad), cubilin and megalin were detected with specific rabbit anti-cubilin and anti-megalin antibodies diluted 1/2,000, and secondary rabbit peroxydase-conjugated antibodies diluted 1/10,000, and visualized with an ECL kit (RPN 2106; Amersham).

Cubilin and megalin expression analysis

RNA was isolated from kidney using the RNA Instapure Kit (Eurogentec), and RT was carried out. Cubilin, megalin, and 18S were quantified in the same RT reactions by real-time PCR (Light Cycler; Roche). The sequences used for detection of murine cubilin-complementary DNA (cDNA) were as follows: sense 5′-CAGACACCCACCATGGATATGA-3′and antisense 5′-TTCGTTGCCCAAAAGAGTCC-3′; cubilin-cDNA was quantified with the Taqman probe 5′-TCTGGGCCTCCTCTCCTACTGGCTG-3′. The following sequences were used for detection of mouse megalin-cDNA: sense 5′-TCCAAAGTGGGCCTGGC-3′ and antisense 5′-TTTTCCACATTTTCTGGTACAGTCA-3′; megalin-cDNA was quantified with the Taqman probe 5′-TGCAGGGACCGTCAGTAAGCTACAG-3′. 18S was quantified using the Taqman probe (Applied Biosystems; 4310893[E]). Cubilin and megalin expression levels were normalized to that of 18S.

Statistical analysis

Results are given as mean ± SEM, and statistically significant differences were determined with Tukey's multiple comparison test after ANOVA, using GraphPad Prism.

RESULTS

ApoA-II is reabsorbed in kidney proximal tubules

Figure 1A, **B** shows that mapoA-II and hapoA-II are reabsorbed in epithelial cells of kidney proximal tubules of control and hapoA-II-transgenic mice, respectively. Because anti-mapoA-II antibody cross-reacted to some degree with hapoA-II, mapoA-II immunostaining in kidney of hapoA-II-transgenic mice is not shown. Intense hapoA-II immunostaining was detected in epithelial cells just below the brush border membrane in λ-transgenic mice (Fig. 1A1), but not in proximal tubules of control mice (Fig. 1A2), showing the specificity of the anti-hapoA-II antibody. ApoA-II was present exclusively in proximal tubules, mainly in the first (S1) segment adjacent to the glomerulus, and was not detected in glomeruli and distal nephron (not shown). As a control, mapoA-I, known to be catabolized in the kidney (13–17), was also immunolocalized only in the S1 segment of kidney proximal tubules of the same mice (not shown). To our knowledge, these data are the first report of apoA-II reabsorption in the kidney.

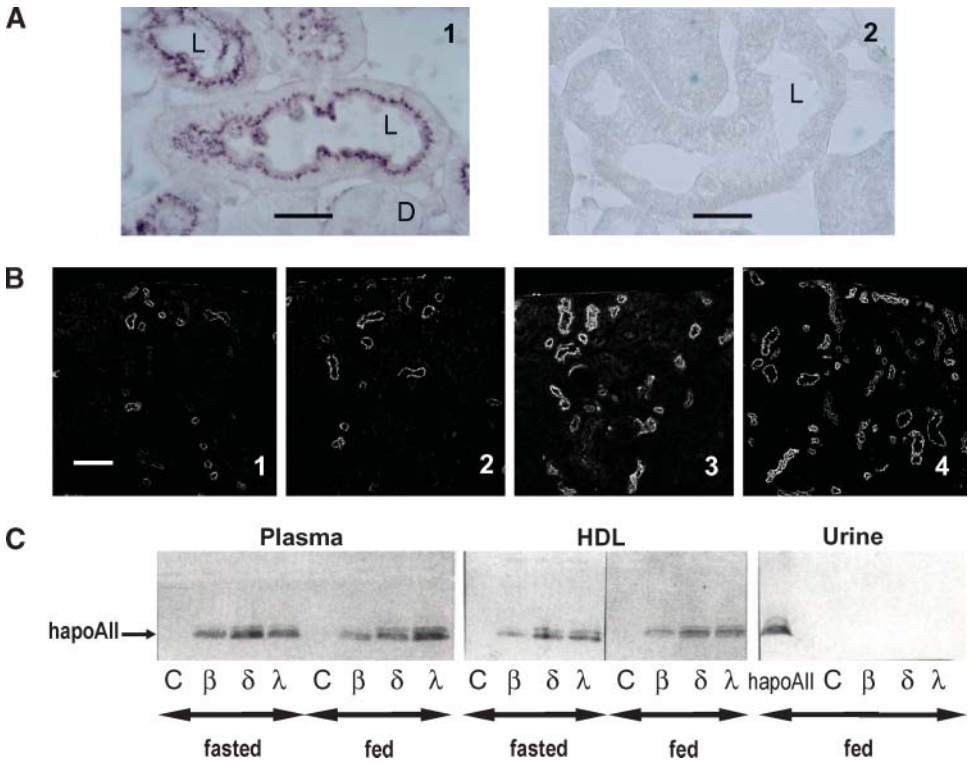

Fig. 1. Apolipoprotein A-II (apoA-II) is reabsorbed in kidney proximal tubules. Kidneys were obtained from control and human apoA-II (hapoA-II) transgenic mice (four to five animals from each genotype), and representative images of kidney sections are shown. Paraffin-embedded kidney sections were analyzed by (**A**) bright-field microscopy, bar: 20 μm; and (**B**) confocal microscopy, bar: 100 μm. (**A**) Immunostaining for hapoA-II in hapoA-II-transgenic λ mice (A1) shows hapoA-II internalization at the apical surface of proximal tubules (L, lumen) but not in distal tubules (D). Conversely, proximal tubules of control mice (A2) are not immunostained with the anti-hapoA-II antibody, confirming that it does not recognize murine apolipoprotein A-II (mapoA-II). (**B**) Immunostaining for mapoA-II in control mice (B1); immunostaining for hapoA-II in transgenic β mice (B2), δ mice (B3), and λ mice (B4). Reabsorption of apoA-II in proximal tubules is directly related to its concentration in plasma. (**C**) Western blot of hapoA-II in whole plasma, HDL, and urine of control and hapoA-II-transgenic mice, either fed ad libitum or fasted overnight. Plasma pools were constituted of equal volumes of EDTA-plasma drawn from the retroorbital plexus of five mice per group, and 5 μl samples (diluted 10 times) were run on the gels. The HDL fractions were isolated by ultracentrifugation from two separate plasma pools, each obtained from 8 to 10 animals, and one representative gel is shown (6 μg HDL-protein per lane). For plasma and HDL, lanes 1 and 5 correspond to control (C) mice, lanes 2 and 6 to β-transgenic mice, lanes 3 and 7 to δ-transgenic mice, and lanes 4 and 8 to λ-transgenic mice. Urine was concentrated 100 times and extensively dialyzed using Amicon Ultra-4 tubes with a 5 kDa cutoff, and 20 μl samples were run on the gels. After SDS-PAGE on 15% gels was performed, proteins were transferred to nitrocellulose membranes and blotted with rabbit anti-hapoA-II antiserum. One representative immunoblot out of two is shown. Lane 1: purified hapoA-II; lanes 2 to 5: urine from ad libitum-fed control (C) β-, δ-, and λ-transgenic mice, respectively. Urine from fasted mice was equally devoid of apoA-II and is not shown.

ApoA-II was totally absent in urine of control and transgenic mice (Fig. 1C), and the same was true for apoA-I (not shown). These observations indicate a highly efficient internalization in proximal tubule epithelial cells of apoA-II and apoA-I filtered through the glomeruli.

ApoA-II colocalizes with apoA-I, cubilin, and megalin, and is targeted to lysosomes of kidney proximal tubules

In these experiments, kidney sections were prepared from the higher-expressing λ mice, and immunostaining of hapoA-II, mapoA-I, cubilin, and megalin was performed. ApoA-II (**Fig. 2A2**), as apoA-I (Fig. 2A1), was present in the apical cytoplasm in punctate form, corresponding to small vesicles, and both apolipoproteins partially colocalized in the same vesicles (Fig. 2A3 and Fig. 2A4). Cubilin (Fig. 2B1) and megalin (Fig. 2C1) were abundantly expressed and lined the entire brush border apical membrane of the tubules, where they colocalized (not shown). Of note, apoA-II partially colocalized with cubilin (Fig. 2B3) and somewhat with megalin (Fig. 2C3) only in the brush border

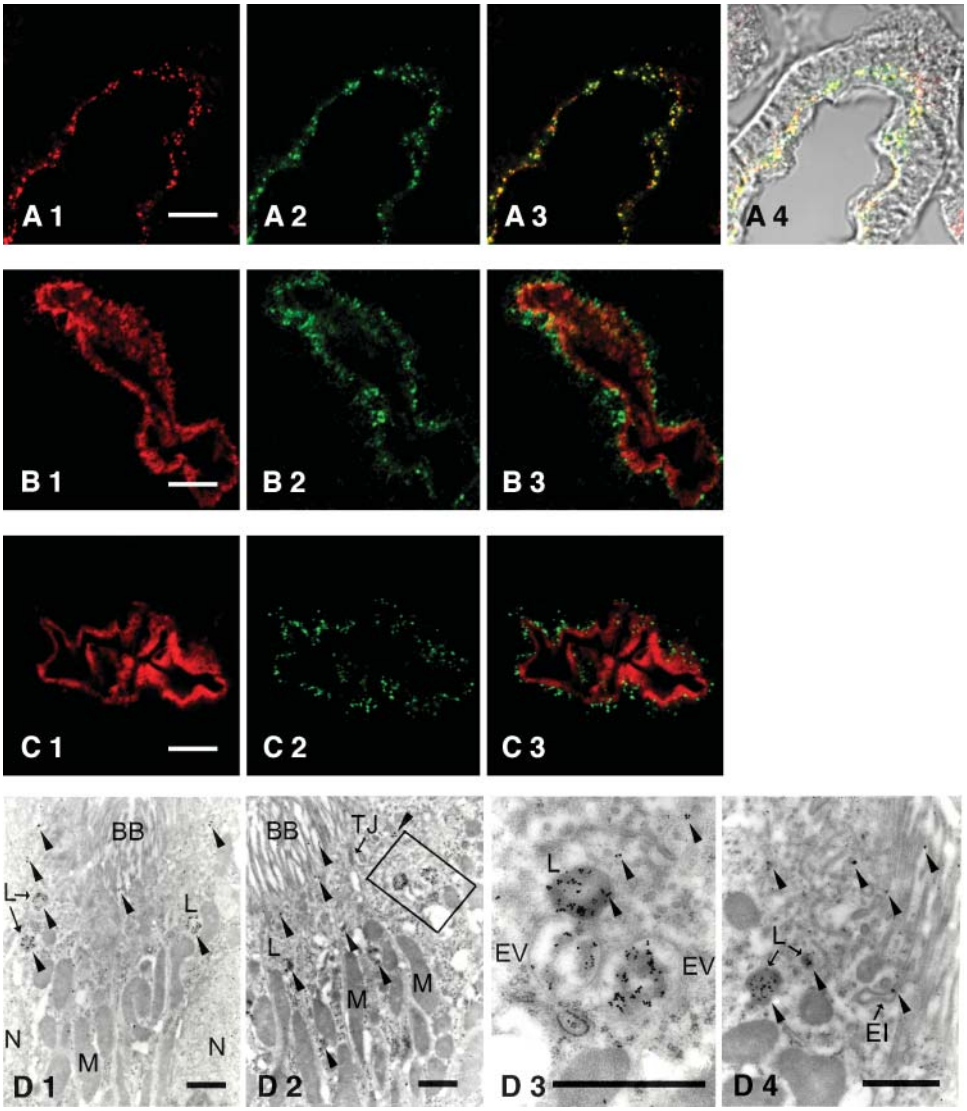

Fig. 2. ApoA-II colocalizes with apoA-I, cubilin, and megalin in kidney proximal tubules and is targeted to lysosomes. (**A–C**) Immunohistochemical localization of hapoA-II, mapoA-I, cubilin, and megalin in kidney proximal tubules of hapoA-II-transgenic λ mice was studied by confocal microscopy. ApoA-II and apoA-I are present in punctate form corresponding to small vesicles just below the apical membrane and partially colocalize in these vesicles (**A**). ApoA-II partially colocalized with cubilin (**B**) and somewhat with megalin (**C**), only in the brush border. (**A**) Immunostaining for mapoA-I (A1), hapoA-II (A2), merge (A3) and merge with phase contrast (Nomarski) showing mapoA-I and hapoA-II internalization in epithelial cells at the apical surface just below the brush border membrane (A4). (**B**) Immunostaining for cubilin (B1), hapoA-II (B2), merge (B3). (**C**) Immunostaining for megalin (C1), hapoA-II (C2), merge (C3). Bars for **A** to **C**: 10 μm. (**D**) Immunogold labeling of hapoA-II (arrowheads) is localized in the brush border (BB), in small endocytic invaginations (EI) at the base of the brush border, in endocytic vacuoles (EV) and is concentrated in lysosomes (L). Three different electronmicrographs of proximal tubules are shown: D1, D2, and D4; D3 is the inset of D2. Bars: 1 μm. N, nucleus; M, mitochondrion; TJ, tight junction.

and was present alone in small vesicles in epithelial cells just below the membrane. Similar results were obtained for apoA-I, which served as a positive control (not shown).

To follow apoA-II trafficking along the endocytic pathway, hapoA-II was detected by immunoelectron microscopy in kidney sections of λ mice. Immunogold apoA-II was present near the brush border membrane, in endocytic invaginations and vacuoles, and was concentrated in lysosomes (Fig. 2D1-D4). The intense apoA-II immunostaining in lysosomes is suggestive of apoA-II degradation in kidney proximal tubules.

Renal catabolism of apoA-II is a function of its plasma concentration

To study the relationship between renal catabolism and plasma level of hapoA-II, we compared the amount of hapoA-II immunostaining in kidney sections from the three hapoA-II transgenic lines β, δ, and λ with plasma hapoA-II concentrations of 20, 40, and 60 mg/dl, respectively (**Table 1**). Furthermore, we modulated plasma hapoA-II by overnight fasting all transgenic lines, because fasting lowers plasma hapoA-II up to 40% in the λ mice (8). Indeed, hapoA-II is lower in total plasma and HDL fractions of fasted as compared with fed transgenic mice (Fig. 1C). In the fed state, the percentage of tubules immunostained for hapoA-II was lowest in β mice and similar between δ and λ mice, despite the higher plasma content of hapoA-II in λ compared with δ mice (Table 1 and Fig. 1B). A possible explanation is that lysosomal degradation of apoA-II proceeds at similar rates in δ and λ mice. In each transgenic line, immunostaining of hapoA-II was consistently lower in fasted compared with fed mice. Immunostaining of cubilin and megalin showed that both proteins were abundantly present in brush border membranes of fed and fasted transgenic and control mice. We also verified that kidney mRNA levels of cubilin and megalin were similar among all genotypes in both the fed and fasted states, indicating that the lower renal uptake of apoA-II in fasted mice could not be due to decreased cubilin and/or megalin expression levels (**Table 2**). Rather, renal apoA-II catabolism is related to circulating apoA-II concentration, suggesting an association between hapoA-II concentration in plasma and reabsorption in the kidney.

TABLE 1. Immunolocalization of endogenous murine apoA-II and human apoA-II in sections of kidney proximal convoluted tubules

Nutritional State	Genotype	MapoA-II[a] in Kidney	HapoA-II[a] in Kidney	HapoA-II[b] in Plasma
				mg/dl
Fed	Controls	8.3 ± 1.1	—	—
	hAIItg-β	—	13.6 ± 1.2	18.6 ± 1.2
	hAIItg-δ	—	30.1 ± 1.9[c]	40.1 ± 1.9[c]
	hAIItg-λ	—	30.4 ± 2.4[c]	60.4 ± 2.4[c]
Fasted	Controls	10.6 ± 1.7	—	—
	hAIItg-β	—	5.5 ± 1.1[d]	17.5 ± 1.1[d]
	hAIItg-δ	—	13.7 ± 1.3[c,d]	30.7 ± 1.3[c,d]
	hAIItg-λ	—	14.2 ± 1.3[c,d]	40.2 ± 1.3[c,d]

Four to five mice from each genotype and nutritional condition were analyzed. Results are given as mean ± SEM. Statistically significant differences were determined by Tukey's multiple comparison test after ANOVA. We did not compare the number of tubules containing immunoreactive mapoA-II with those containing immunoreactive hapoA-II because different antibodies were used.

[a] Immunoenzymatic histological sections from kidney cortex were observed at ×25 power field. For each group of mice, 20 random fields were analyzed in a semi-quantitative manner: the number of total tubules and of tubules containing immunoreactive mapoA-II and hapoA-II were counted, and the results represent the percentage of apolipoprotein-containing tubules.

[b] The plasma concentration of hapoA-II of all transgenic mice used in this study was measured by immunonephelometry as described in Materials and Methods and is expressed in mg/dl.

[c] $P < 0.001$ between the lower-expressing transgenic β mice and the higher-expressing δ and λ mice, under the same nutritional conditions.

[d] $P < 0.001$ between fed and fasted mice of the same genotype.

Uptake of apoA-II by rat yolk sac cells expressing cubilin and megalin is inhibited by apoA-I, HDL, LDL, and anti-cubilin antibodies

To further explore whether cubilin mediates endocytosis of apoA-II, we used rat yolk sac epithelial BN cells (**Fig. 3**), which abundantly express cubilin and its tandem receptor, megalin (**Fig. 4A**). After 1 h incubation at 4°C with Alexa-apoA-II (Fig. 3A2), we observed a uniformly distributed punctate surface staining, which colocalized with the staining for cubilin (Fig. 3A3) and megalin (not shown). Alexa-apoA-II was internalized in BN cells from 1 min onwards and was present in small endocytic vesicles. Incubation of BN cells with unlabeled hapoA-II (which was detected by immunocytochemical techniques, as in kidney sections) resulted in the same internalization pattern as Alexa-apoA-II (not shown). As a control, apoA-I was incubated in parallel experiments with BN cells, with the same results (not shown). Figure 3B shows internalization of Alexa-apoA-II and Alexa-apoA-I in small intracellular vesicles after 5 min incubation at 37°C, as well as their colocalization in the same vesicles. The internalization of Alexa-apoA-I was completely blocked by the addition of excess unlabeled apoA-II (Fig. 3C2). Reciprocally, the internalization of Alexa-apoA-II was completely blocked by the addition of excess unlabeled apoA-I (Fig. 3D2). These findings are a strong indication that apoA-II is internalized by the same receptor system as apoA-I. Furthermore, HDL was the most

TABLE 2. Relative mRNA contents of mouse cubilin and megalin in kidney

Nutritional State	Genotype	Cubilin	Megalin
Fed	Controls	178.8 ± 20.9	234.2 ± 34.3
	hAIItg-β	198.8 ± 11.4	297.5 ± 20.8
	hAIItg-δ	186.8 ± 27.4	208.8 ± 31.8
	hAIItg-λ	197.2 ± 15.0	260.0 ± 43.2
Fasted	Controls	107.8 ± 37.7	140.0 ± 60.2
	hAIItg-β	155.5 ± 9.3	195.7 ± 12.8
	hAIItg-δ	138.5 ± 18.3	180.5 ± 24.4
	hAIItg-λ	171.5 ± 21.9	200.0 ± 19.0

Results are expressed in arbitrary units as the ratios of mRNAs of cubilin and megalin to 18S, and are the mean ± SEM for four to six animals per group. The results were analyzed by ANOVA followed by Tukey's multiple comparison test. Differences among experimental groups were not statistically significant.

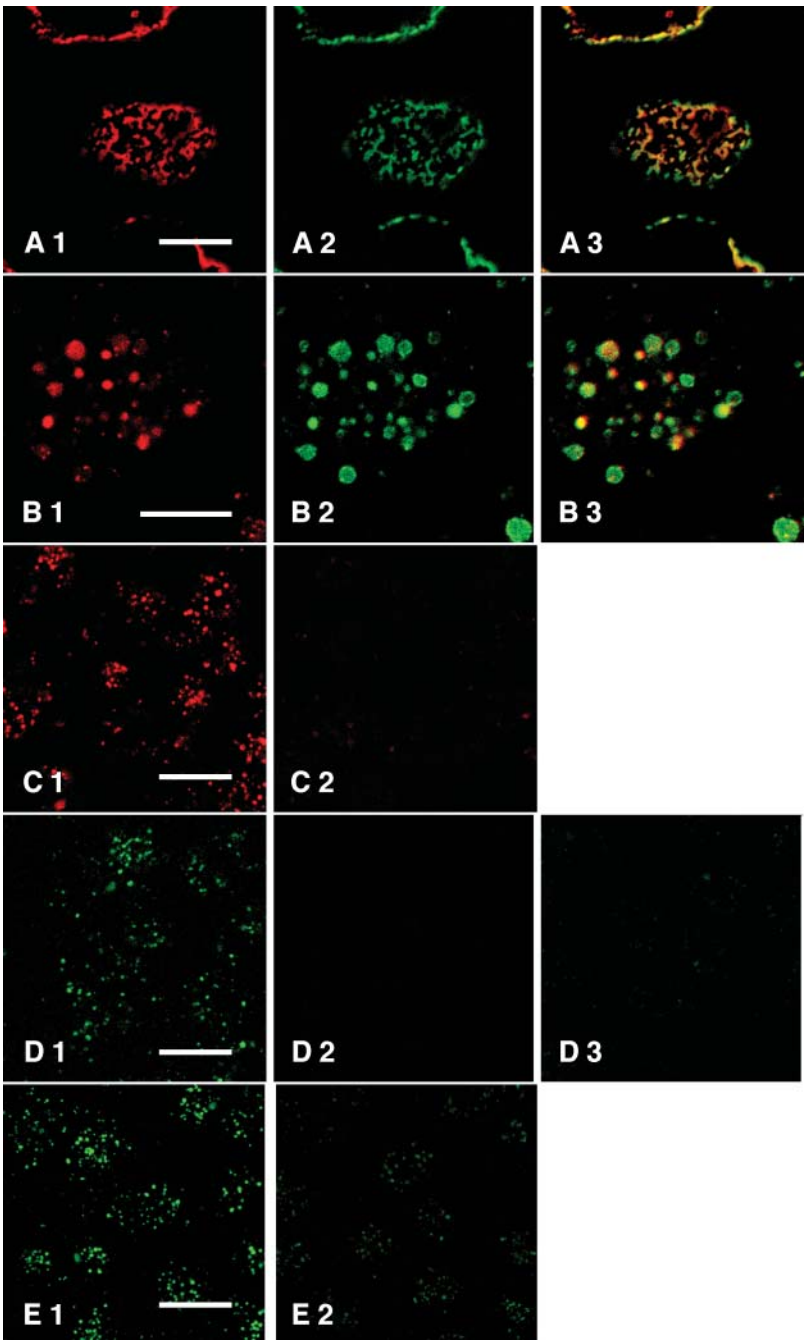

Fig. 3. Uptake of apoA-II by yolk sac cells is inhibited by apoA-I, HDL, LDL, and anti-cubilin antibodies. Uptake of hapoA-II by brown Norwegian (BN) rat yolk sac cells (BN cells) was analyzed by confocal microscopy. (**A**) BN cells were incubated with 2 μg/ml Alexa 488-apoA-II at 4°C for 1 h, and then with rabbit anti-cubilin antibodies, as described in Materials and Methods; immunostaining for cubilin (A1), hapoA-II (A2), merge (A3). ApoA-II colocalized with cubilin at the cell surface. (**B**) BN cells were incubated with Alexa 488-apoA-II and Alexa-546-apoA-I (2 μg/ml of each) at 37°C for 5 min; hapoA-I (B1), hapoA-II (B2), merge (B3). ApoA-II and apoA-I are internalized and partially colocalize in intracellular vesicles. (**C**) BN cells were incubated with 0.25 μg/ml Alexa-546-apoA-I at 37°C for 5 min alone (C1), and in the presence of 500 μg/ml unlabeled hapoA-II (C2). ApoA-II in excess completely blocks apoA-I internalization. (**D**) BN cells were incubated with 0.25 μg/ml Alexa-448-apoA-II at 37°C for 5 min alone (D1), in the presence of 500 μg/ml unlabeled hapoA-I (D2), and in the presence of 200 μg/ml unlabeled HDL (D3). ApoA-I and HDL in excess completely block apoA-II internalization. (**E**) BN cells were incubated at 37°C for 10 min with 100 μg/ml control IgG (E1) or with 100 μg/ml anti-cubilin IgG (E2), and then with 0.25 μg/ml Alexa-448-apoA-II at 37°C for 5 min. ApoA-II internalization was decreased by anti-cubilin antibodies. Bars for **A** and **B**: 10 μm; bars for **C**, to **E**: 20 μm.

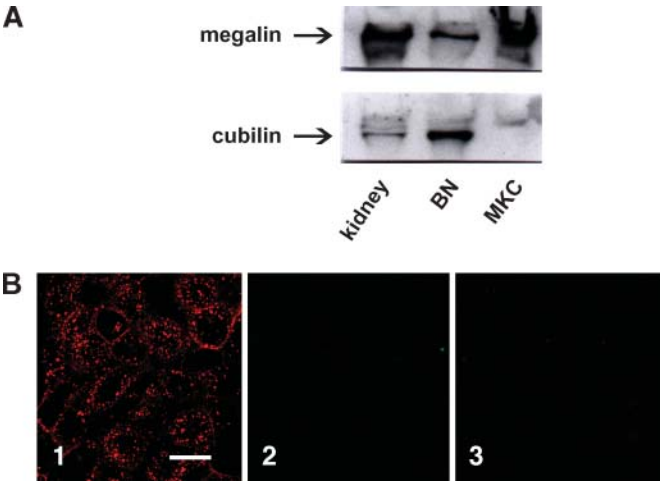

Fig. 4. Kidney cortical cells do not internalize apoA-II and A-I. (**A**) Western blot of cubilin and megalin in kidney, BN yolk sac cells, and mouse kidney cortical cells (MKC cells). Membrane proteins (10 μg for kidney and yolk sac cells and 86 μg for kidney cortical cells) were subjected to 4–15% SDS-PAGE followed by immunoblotting with rabbit anti-megalin and anti-cubilin antibodies. Note that cubilin is totally absent in MKC cells. (**B**) MKC cells were incubated at 37°C for 15 min with 4 μg/ml 1,1'-dioctadecyl-3,3,3′,3′-tetramethylindocarbocyanine-LDL (1), for 2 h with 2 μg/ml Alexa-448-apoA-II (2), and for 2 h with Alexa-546-apoA-I (3). LDL is efficiently internalized, but neither apoA-II nor apoA-I are internalized in MKC cells. Bars: 20 μm.

efficient competitor for internalization of Alexa-apoA-II (Fig. 3D3) and Alexa-apoA-I (not shown). LDL, which is taken up by megalin via binding to apoB-100 (31), competed less efficiently for uptake with Alexa-apoA-II and Alexa-apoA-I (not shown). LDL may decrease apoA-II and A-I uptake by partially sequestering megalin. These results indicate that apoA-II uptake by yolk sac cells may be mediated by cubilin, potentially acting in cohort with megalin.

To directly test the role of cubilin as an endocytic apoA-II receptor, anti-cubilin antibodies were evaluated for their ability to block Alexa-apoA-II internalization in BN cells. Indeed, apoA-II internalization was decreased in the presence of anti-cubilin antibodies (Fig. 3E2). Alexa-apoA-II internalization was estimated as the sum of the IOD of each slice of stack images of the cells, and was decreased by 40% in the presence of anti-cubilin IgG [7,158 ± 611 × 10^3 IOD (n = 4) and 11,770 ± 1,039 × 10^3 IOD (n = 4) in the presence of anti-cubilin IgG and control IgG, respectively]. A similar inhibition of Alexa-apoA-I internalization was obtained by anti-cubilin IgG (not shown).

Lack of apoA-II and apoA-I internalization in megalin-expressing MKC cells

To assess whether megalin is sufficient to mediate apoA-II and apoA-I endocytosis, we used MKC cells expressing megalin but not cubilin. We first established that the megalin mRNA amount of MKC cells was comparable to that of kidney, whereas cubilin mRNA was not detected (not shown). Western blot analysis of total membrane proteins revealed the presence of megalin and the complete absence of cubilin in MKC cells (Fig. 4A). These results were confirmed by immunohistochemistry of MKC cells using anti-megalin and anti-cubilin antibodies (not shown). We then showed that DiI-LDL was taken up efficiently, establishing that megalin was functional (Fig. 4B1). However, neither Alexa-apoA-II nor Alexa-apoA-I was internalized in MKC cells (Fig. 4B2 and 4B3, respectively). Thus, megalin alone cannot internalize apoA-II and apoA-I.

DISCUSSION

We show for the first time, to our knowledge, that apoA-II, the second most abundant HDL apolipoprotein, is catabolized in the kidney. ApoA-II was efficiently internalized in epithelial cells of the first segment of kidney proximal tubules and was concentrated in lysosomes, indicative of degradation. Renal apoA-II reabsorption was associated with its plasma concentration, suggesting that a similar fraction of apoA-II is cleared in the kidney at any given moment. ApoA-II uptake, like that of apoA-I, may be mediated by cubilin and its tandem receptor, megalin. Megalin alone cannot mediate uptake of apoA-II.

This study shows that apoA-II shares renal clearance with apoA-I, the major HDL apolipoprotein, and provides physiologically relevant data for in vivo apoA-II catabolism in the kidney. Indeed, endogenous unlabeled mapoA-II and hapoA-II were detected by immunohistochemistry in proximal tubules of control and hapoA-II-transgenic mice, respectively. As a positive control, native mapoA-I was immunolocalized in proximal tubules of all mice. Previous studies of in vivo apoA-I catabolism after injection of ^{125}I-apoA-I-HDL into rats, rabbits, and mice detected ^{125}I-apoA-I in tissue homogenates, either primarily in kidney (13) or in liver (14). However, it was shown in rabbits that ^{125}I-apoA-I did not behave in vivo as unlabeled apoA-I in terms of tissue uptake: endogenous apoA-I was catabolized predominantly in the kidney, whereas about half of ^{125}I-apoA-I was catabolized in the kidney and half in the liver (15). We therefore avoided labeling apoA-II with ^{125}I in this study, and instead, opted for immunolocalization of native endogenous apoA-II in kidney sections. The observation that apoA-II and apoA-I were reabsorbed in the first segment of proximal tubules and were totally absent in urine suggests a very efficient uptake, as in the case of IF (23). Internalization of apoA-II was followed by its targeting to lysosomes, suggestive of degradation, and similarly to transferrin, albumin, and IF (23).

The use of three hapoA-II-transgenic mouse lines with a gradient of hapoA-II expression allowed us to show that apoA-II reabsorption in the kidney is related to its plasma concentration. The decrease in plasma hapoA-II resulting from fasting was also accompanied by a decrease in apoA-II content in the kidney. On the other hand, cubilin and megalin were abundantly present in brush border membranes of fed and fasted mice of all genotypes, and their mRNAs were similar. Taken together, these observations suggest that plasma apoA-II concentration is regulated by its rate of synthesis and not by its rate of catabolism, in accordance with apoA-II turnover studies (11).

A major question arising from the present data is whether apoA-II is cleared in the kidney in lipid-poor form or associated with HDL. Because of its high hydrophobicity, hapoA-II binds tightly to the surface phospholipids of HDL, and it is not known whether part of apoA-II circulates in plasma in lipid-poor form, as does apoA-I (17). Furthermore, we did not detect apoA-II in the lipoprotein-deficient fraction ($d > 1.21$ g/l) of human or murine plasma (unpublished observations). In our transgenic mice, hapoA-II associates with both large (10 nm) and small (7.8 nm) HDL particles, the latter predominant in the high-expressing λ mice (7, 8). It remains indeterminate whether in vivo HDL holoparticles filter through the glomerulus. At present, we can only speculate that some small HDL particles carrying hapoA-II may filter through the glomerulus and be reabsorbed in the proximal tubules. Regarding apoA-I, it is probably reabsorbed in kidney in lipid-poor form (13), and an inverse relationship has been demonstrated between serum-free apoA-I levels and glomerular filtration rates in patients with renal failure (17).

An important issue concerns the proteins/receptors mediating apoA-II internalization in kidney proximal tubules. Based on several lines of evidence obtained in vivo and in vitro, the present data indicate that cubilin may be an apoA-II receptor in the kidney, although they do not exclude the existence of other apoA-II receptors. Native apoA-II taken up in vivo was detected in kidney sections by immunostaining, and colocalized to a great extent with apoA-I, an established cubilin ligand, in endocytic vesicles below the brush border membrane of tubular epithelial cells. ApoA-II was internalized only in proximal tubules, mainly in the S1 segment adjacent to the glomeruli, where cubilin and megalin are abundantly expressed, and was not detected in distal or collecting tubules, where cubilin and megalin are not expressed (23). This pattern of internalization is similar to that reported for known ligands of the cubilin-megalin complex (23). Conversely, cubilin and megalin were not detected in intracellular vesicles by confocal microscopy, suggesting that they rapidly recycle to the apical membrane from an early endosomal compartment. Indeed, electon microscopic studies clearly showed cubilin and megalin colocalization on the luminal membrane, in endocytic compartments, and in the recycling compartment dense apical tubules (23). In yolk sac epithelial cells with abundant cubilin expression, apoA-II colocalized to a great extent with cubilin at the cell surface, as did apoA-I. More importantly, both apolipoproteins competed equally efficiently with each other for uptake, and uptake of apoA-II was very efficiently blocked by HDL. Moreover, apoA-II internalization was inhibitable by anti-cubilin antibodies, to the same extent as apoA-I internalization. Previously, Hammad et al. (19) showed that HDL endocytosis by cubilin- and megalin-expressing endoderm-like F9 cells was inhibitable by apoA-II. Conversely, MKC cells that express megalin but not cubilin do not internalize apoA-II and apoA-I, in agreement with the Hammad et al. (22) report that megalin did not bind HDL, delipidated HDL, or apoA-I.

Our results clearly show that megalin is not an apoA-II and apoA-I receptor. The similarities of apoA-I and apoA-II uptake suggest that cubilin is their common receptor. However, cubilin requires megalin as a coreceptor for ligand internalization; and a second accessory protein, amnionless (AMN), that binds to its amino-terminal third, ensures cubilin trafficking to the cell surface, and directs subcellular localization and endocytosis of cubilin and its ligands (32, 33). Fyfe et al. (32) have therefore proposed the existence of a functional complex of cubilin/AMN named "cubam." AMN is expressed in the same tissues as cubilin and megalin and is also expressed in the BN yolk sac cells used in the present study (P. Verroust, unpublished observations). Thus, our results are equally well explained by binding of apoA-II to cubilin or to cubam, whereas internalization necessitates megalin, as demonstrated by several studies.

This study did not address the relative uptake of apoA-II in the kidney compared with any other organ. If apoA-II is mainly catabolized as an HDL component, it may share with apoA-I other sites of catabolism. When ^{125}I-apoA-I-HDL was injected in vivo, ^{125}I-apoA-I was detected primarily in tissue homogenates of kidney, ovary, and adrenal, and in lesser proportions in liver and spleen (13). It is noteworthy that the relative proportions of ^{125}I-apoA-I-HDL taken up by kidney and liver vary among studies; in some studies, uptake is greater in kidney (13, 15, 34), and in other studies, in liver (14, 35). A study using independently generated hapoA-II-transgenic mice showed an increased ^{125}I-apoA-I-HDL catabolism in kidney in the high-expressing 11.1 line, compared with the low-expressing 25.3 transgenic line or with control mice (34). The greater apoA-I catabolism in 11.1 transgenic mice was attributed to the displacement of mapoA-I from HDL by the more hydrophobic hapoA-II, and to the generation of smaller HDL particles (reproduced in vitro). On the other hand, HDL-apoA-I catabolism in liver and kidney was comparable between wild-type and scavenger receptor class B type I (SR-BI) knockout mice (35). A 95 kDa high-affinity HDL binding protein, which binds HDL_3, apoA-I, and apoA-II, has been characterized in hepatic and nonhepatic cell lines (36). Another important tissue for HDL uptake is the developing embryo, in which cholesterol is essential for growth as well as for steroid hormone synthesis by embryonic and extraembryonic tissues. HDL-cholesterol is particularly important in rodents that have low plasma levels of remnants/LDL. The visceral yolk sac epithelium is the functional fetal-maternal barrier and takes up maternal lipoproteins via several receptors: LDL-receptor, cubilin, megalin, and AMN, SR-BI, with finely tuned temporal expression patterns for each receptor (37–40). Cubilin is expressed very early on the apical surface of yolk sac, before SR-BI [expressed on day 10.5 (37)], and its deficiency in cubilin-knockout embryos completely inhibited DiI-HDL uptake at day 8.0 (40). At day 10.5, HDL-apoA-I and HDL-cholesteryl esther were cleared at equally very high rates in the yolk sac, indicating that the whole HDL particle was internalized (38). HDL holoparticle uptake may thus be mediated by cubilin, already expressed

in the yolk sac on day 8.0 (40), whereas SR-BI mediates selective HDL-cholesterol uptake (37). Because cubilin has a restricted pattern of expression (kidney proximal tubules, distal small intestine, and visceral endoderm of the embryo), other receptor pathways for apoA-II are expected to be operative in other organs. Further in vivo studies are needed to investigate apoA-II catabolism in organs besides kidney, to identify the receptors involved, and to estimate the relative contributions of individual organs to apoA-II catabolism.

In conclusion, the present data demonstrate for the first time a physiologically relevant clearance of apoA-II in the kidney, which occurred in relation to plasma apoA-II concentration. ApoA-II reabsorption in kidney proximal tubules is probably mediated by cubilin, like that of apoA-I, and is probably followed by degradation in lysosomes. Future studies will address the question of whether apoA-II is cleared in the kidney in a lipid-poor form or as a component of HDL subclasses, as well as the role of other organs in apoA-II catabolism. Our transgenic mouse models expressing hapoA-II at various levels will be useful for gaining insight into the in vivo role of apoA-II in HDL remodeling and catabolism, which are important parameters underlying the protective actions of HDL on cardiovascular artery disease.

We acknowledge the financial support of the Institut National de la Santé et de la Recherche Médicale (Inserm). S. Dugué-Pujol and X. Rousset are recipients of a doctoral fellowship from the Ministère de la Recherche et Technologie (France). The authors thank Dr. O. Kellermann for providing a mouse transgenic for a recombinant plasmid adeno-SV40 (PK4), from which a mouse kidney cortex epithelial cell (MKC) culture was developed. We also thank Dr. Josiane Poggioli and Françoise Grelac (Inserm U356, Paris, F-75006) for providing MKC cells. We are grateful to Dr. Martine Pinçon-Raymond for helpful advice with immunoelectron microscopy. We wish to thank Carole Lasne and Maryse Séau for excellent technical assistance.

REFERENCES

1. Williamson, R., D. Lee, J. Hagaman, and N. Maeda. 1992. Marked reduction of high density lipoprotein cholesterol in mice genetically modified to lack apolipoprotein A-I. *Proc. Natl. Acad. Sci. USA.* **88:** 7134–7138.
2. Weng, W., and J. L. Breslow. 1996. Dramatically decreased high density lipoprotein cholesterol, increased remnant clearance, and insulin hypersensitivity in apolipoprotein A-II knockout mice suggest a complex role for apolipoprotein A-II in atherosclerosis susceptibility. *Proc. Natl. Acad. Sci. USA.* **93:** 14788–14794.
3. Lagocki, P. A., and A. M. Scanu. 1980. In vitro modulation of the apolipoprotein composition of high density lipoprotein. Displacement of apolipoprotein A-I from high density lipoprotein by apolipoprotein A-II. *J. Biol. Chem.* **255:** 3701–3706.
4. Durbin, D. M., and A. Jonas. 1997. The effect of apolipoprotein A-II on the structure and function of apolipoprotein A-I in a homogeneous reconstituted high density lipoprotein particle. *J. Biol. Chem.* **272:** 31333–31339.
5. Boisfer, E., G. Lambert, V. Atger, N. Q. Tran, D. Pastier, C. Benetollo, J-F. Trottier, I. Beaucamps, M. Antonucci, M. Laplaud, et al. 1999. Overexpression of human apolipoprotein A-II in mice induces hypertriglyceridemia due to defective very low density lipoprotein hydrolysis. *J. Biol. Chem.* **274:** 11564–11572.
6. Pastier, D., S. Dugué, E. Boisfer, V. Atger, N. Q. Tran, A. van Tol, M. J. Chapman, J. Chambaz, P. M. Laplaud, and A. D. Kalopissis. 2001. Apolipoprotein A-II/A-I ratio is a key determinant in vivo of HDL concentration and formation of pre-beta HDL containing apolipoprotein A-II. *Biochemistry.* **40:** 12243–12253.
7. Rye, K-A., K. Wee, L. K. Curtiss, D. J. Bonnet, and P. J. Barter. 2003. Apolipoprotein A-II inhibits high density lipoprotein remodeling and lipid-poor apolipoprotein A-I formation. *J. Biol. Chem.* **278:** 22530–22536.
8. Weng, W., N. A. Brandenburg, S. Zhong, J. Halkias, L. Wu, X-C. Jiang, A. Tall, and H. L. Breslow. 1999. ApoA-II maintains HDL levels in part by inhibition of hepatic lipase: studies in apoA-II and hepatic lipase double knockout mice. *J. Lipid Res.* **40:** 1064–1070.
9. Miller, G. J., and N. E. Miller. 1975. Plasma-high-density-lipoprotein concentration and development of ischaemic heart-disease. *Lancet.* **1:** 16–19.
10. Koro, C. E., S. J. Bowlin, T. E. Stump, D. L. Sprecher, and W. M. Tierney. 2006. The independent correlation between high-density lipoprotein cholesterol and subsequent major adverse coronary events. *Am. Heart J.* **151:** 755.e1–755.e6.
11. Ikewaki, K., L. A. Zech, M. Kindt, H. B. Brewer, Jr., and D. J. Rader. 1995. Apolipoprotein A-II production rate is a major factor regulating the distribution of apolipoprotein A-I among HDL subclasses LpA-I and LpA-I:A-II in normolipidemic humans. *Arterioscler. Thromb. Vasc. Biol.* **15:** 306–312.
12. Hussain, M. M., and V. I. Zannis. 1990. Intracellular modification of human apolipoprotein AII (apoAII) and sites of apoAII mRNA synthesis: comparison of apoAII with apoCII and apoCIII isoproteins. *Biochemistry.* **29:** 209–217.
13. Glass, C. K., R. C. Pittman, G. A. Keller, and D. Steinberg. 1983. Tissue sites of degradation of apoprotein A-I in the rat. *J. Biol. Chem.* **258:** 7161–7167.
14. Glass, C. K., R. C. Pittman, M. Civen, and D. Steinberg. 1985. Uptake of high-density lipoprotein-associated apoprotein A-I and cholesterol esters by 16 tissues of the rat in vivo and by adrenal cells and hepatocytes in vitro. *J. Biol. Chem.* **260:** 744–750.
15. Braschi, S., T. A-M. Neville, C. Maugeais, T. A. Ramsamy, R. Seymour, and D. L. Sparks. 2000. Role of the kidney in regulating the metabolism of HDL in rabbits: evidence that iodination alters the catabolism of apolipoprotein A-I by the kidney. *Biochemistry.* **39:** 5441–5449.
16. Horowitz, B. S., I. J. Goldberg, J. Merab, T. M. Vanni, R. Ramakrishnan, and H. N. Ginsberg. 1993. Increased plasma and renal clearance of an exchangeable pool of apolipoprotein A-I in subjects with low levels of high density lipoprotein cholesterol. *J. Clin. Invest.* **91:** 1743–1752.
17. Neary, R. H., and E. Gowland. 1988. The effect of renal failure and haemodialysis on the concentration of free apolipoprotein A-I in serum and the implications for the catabolism of high-density lipoproteins. *Clin. Chim. Acta.* **171:** 239–246.
18. Kozyraki, R., J. Fyfe, M. Kristiansen, C. Gerdes, C. Jacobsen, S. Cui, E. I. Christensen, M. Aminoff, A. de la Chapelle, R. Krahe, et al. 1999. The intrinsic factor-vitamin B_{12} receptor, cubilin, is a high-affinity apolipoprotein A-I receptor facilitating endocytosis of high-density lipoprotein. *Nat. Med.* **5:** 656–661.
19. Hammad, S. M., S. Stefansson, W. O. Twal, C. J. Drake, P. Fleming, A. Remaley, H. B. Brewer, Jr., and W. S. Argraves. 1999. Cubilin, the endocytic receptor for intrinsic factor-vitamin B_{12} complex, mediates high density lipoprotein holoparticle endocytosis. *Proc. Natl. Acad. Sci. USA.* **96:** 10158–10163.
20. Moestrup, S. K., and R. Kozyraki. 2000. Cubilin, a high-density lipoprotein receptor. *Curr. Opin. Lipidol.* **11:** 133–140.
21. Moestrup, S. K., R. Kozyraki, M. Kristiansen, J. H. Kaysen, H. H. Rasmussen, D. Brault, F. Pontillon, F. O. Goda, E. I. Christensen, T. G. Hammond, et al. 1998. The intrinsic factor-vitamin B12 receptor and target of teratogenic antibodies is a megalin-binding peripheral membrane protein with homology to developmental proteins. *J. Biol. Chem.* **273:** 5235–5242.
22. Hammad, S. A., J. L. Barth, C. Knaak, and W. S. Argraves. 2000. Megalin acts in concert with cubilin to mediate endocytosis of high density lipoproteins. *J. Biol. Chem.* **275:** 12003–12008.
23. Christensen, E. I., and H. Birn. 2002. Megalin and cubilin: multifunctional endocytic receptors. *Nat. Rev. Mol. Cell Biol.* **3:** 258–268.
24. Lowry, O. H., N. J. Rosebrough, A. L. Farr, and R. J. Randall. 1951. Protein measurement with the folin phenol reagent. *J. Biol. Chem.* **193:** 265–275.
25. Teupser, D., J. Thierry, A. Walli, and D. Seidel. 1996. Determination

of LDL- and scavenger-receptor activity in adherent and non-adherent cultured cells with a new single-step fluorometric assay. *Biochim. Biophys. Acta.* **1303:** 193–198.
26. Laemmli, U. K. 1970. Cleavage of structural proteins during the assembly of the head of bacteriophage T4. *Nature.* **227:** 680–685.
27. Sahali, D., N. Mulliez, F. Châtelet, C. Laurent-Winter, D. Citadelle, J. C. Sabourin, C. Roux, P. Ronco, and P. Verroust. 1993. Comparative immunochemistry and ontogeny of two closely related coated pit proteins. The 280-kd target of teratogenic antibodies and the 330-kd target of nephritogenic antibodies. *Am. J. Pathol.* **142:** 1654–1667.
28. Le Panse, S., M. Galceran, F. Pontillon, B. Lelongt, M. van de Putte, P. M. Ronco and P. J. Verroust. 1995. Immunofunctional properties of a yolk sac epithelial cell line expressing two proteins gp280 and gp330 of the intermicrovillar area of proximal tubule cells: inhibition of endocytosis by the specific antibodies. *Eur. J. Cell Biol.* **67:** 120–129.
29. Chalumeau, C., D. Lamblin, S. Bourgeois, P. Borensztein, R. Chambrey, P. Bruneval, J. P. Duong Van Huyen, M. Froissart, J. Biber, M. Paillard, et al. 1999. Kidney cortex cells derived from SV40 transgenic mice retain intrinsic properties of polarized proximal tubule cells. *Kidney Int.* **56:** 559–570.
30. Thorens, B., J. S. Flier, H. F. Lodish, and B. B. Kahn. 1990. Differential regulation of two glucose transporters in rat liver by fasting and refeeding and by diabetes and insulin treatment. *Diabetes.* **39:** 712–719.
31. Stefansson, S., D. A. Chappell, K. M. Argraves, D. K. Strickland, and W. S. Argraves. 1995. Glycoprotein 330/low density lipoprotein receptor-related protein-2 mediates endocytosis of low density lipoproteins via interactions with apolipoprotein B100. *J. Biol. Chem.* **270:** 19417–19421.
32. Fyfe, J. C., M. Madsen, P. Hojrup, E. I. Christensen, S. M. Tanner, A. de la Chapelle, Q. He, and S. K. Moestrup. 2004. The functional cobalamin (vitamin B_{12})-intrinsic factor receptor is a novel complex of cubilin and amnionless. *Blood.* **103:** 1573–1579.
33. Strope, S., R. Rivi, T. Metzger, K. Manova, and E. Lacy. 2004. Mouse amnionless, which is required for primitive streak assembly, mediates cell-surface localization and endocytic function of cubilin on visceral endoderm and kidney proximal tubules. *Development.* **131:** 4787–4795.
34. Julve, J., J. C. Escolà-Gil, V. Ribas, F. Gonzalez-Sastre, J. Ordonez-Llanos, J. L. Sanchez-Quesada, and F. Blanco-Vaca. 2002. Mechanisms of HDL deficiency in mice overexpressing human apo A-II. *J. Lipid Res.* **43:** 1734–1742.
35. Brundert, M., A. Ewert, J. Heeren, B. Behrendt, R. Ramakrishnan, H. Greten, M. Merkel, and F. Rinninger. 2005. Scavenger receptor class B type I mediates the selective uptake of high-density lipoprotein-associated cholesteryl ester by the liver in mice. *Arterioscler. Thromb. Vasc. Biol.* **25:** 143–148.
36. Bocharov, A. V., T. G. Vishnyakova, I. N. Baranova, A. P. Patterson, and T. L. Eggerman. 2001. Characterization of a 95 kDa high affinity human high density lipoprotein-binding protein. *Biochemistry.* **40:** 4407–4416.
37. Hatzopoulos, A. K., A. Rigotti, R. D. Rosenberg, and M. Krieger. 1998. Temporal and spatial pattern of expression of the HDL receptor SR-BI during murine embryogenesis. *J. Lipid Res.* **39:** 495–508.
38. Wyne, K. L., and L. A. Woollett. 1998. Transport of maternal LDL and HDL to the fetal membranes and placenta of the Golden Syrian hamster is mediated by receptor-dependent and receptor-independent processes. *J. Lipid Res.* **39:** 518–530.
39. McConihay, J. A., A. M. Honkomp, N. A. Granholm, and L. A. Woollett. 2000. Maternal high density lipoproteins affect fetal mass and extra-embryonic fetal tissue sterol metabolism in the mouse. *J. Lipid Res.* **41:** 424–432.
40. Smith, B. T., J. C. Mussell, P. A. Fleming, J. L. Barth, D. D. Spyropoulos, M. A. Cooley, C. J. Drake, and W. S. Argraves. 2006. Targeted disruption of cubilin reveals essential developmental roles in the structure and function of endoderm and in somite formation. *BMC Dev. Biol.* **6:** 30–42.